



**HAL**  
open science

## Circular Polarization in Nature: Factual, Theoretical and Experimental Summary

Serge Berthier, Magali Thomé, Priscilla Simonis

► **To cite this version:**

Serge Berthier, Magali Thomé, Priscilla Simonis. Circular Polarization in Nature: Factual, Theoretical and Experimental Summary. *Materials Today: Proceedings*, 2014, 1, Supplement, pp.145 - 154. 10.1016/j.matpr.2014.09.015 . hal-01236756

**HAL Id: hal-01236756**

**<https://hal.science/hal-01236756>**

Submitted on 2 Dec 2015

**HAL** is a multi-disciplinary open access archive for the deposit and dissemination of scientific research documents, whether they are published or not. The documents may come from teaching and research institutions in France or abroad, or from public or private research centers.

L'archive ouverte pluridisciplinaire **HAL**, est destinée au dépôt et à la diffusion de documents scientifiques de niveau recherche, publiés ou non, émanant des établissements d'enseignement et de recherche français ou étrangers, des laboratoires publics ou privés.



Distributed under a Creative Commons Attribution - NonCommercial - NoDerivatives 4.0  
International License

Living Light: Uniting biology and photonics – A memorial meeting in honour of Prof Jean-Pol Vigneron

## Circular polarization in nature: factual, theoretical and experimental summary

Serge Berthier<sup>a,b,\*</sup>, Magali Thomé<sup>b</sup>, Priscilla Simonis<sup>c</sup>

<sup>a</sup>Université Paris Diderot, 5 rue Thomas-Mann, 75013 Paris, France – UNESCO-UNISA chair in nanotechnology, Cap Town, South Africa.

<sup>b</sup>Institut des NanoSciences de Paris, UMR 7588, 4 Place Jussieu, 75005 Paris, France.

<sup>c</sup>Biophotonic Group, Solid State Physics Lab. Research Center in Physics of Matter and Radiation (PMR)  
Université de Namur, Rue de Bruxelles 61 - 5000 Namur, Belgique

---

### Abstract

Circular polarization of light created by living organisms has recently been the subject of renewed interest. At the origin is the discovery, in a marine arthropod, of a visual device sensitive to this state and able to distinguish the left circular polarization from the right one. Numerous other organisms that produce circularly polarized light by reflection, mainly beetles of the Scarabaeidae family, have also been identified and biologists now want to test their sensitivity to this polarization state. Along with this, the experimental techniques used to characterize the polarization states of light, as well as the structures that generate them, have significantly evolved. We present here the different sources of circular polarization found in nature, animal origin or not, as well as the theoretical bases for their study. Different experimental techniques are then quickly presented.

© 2014 The Authors. Published by Elsevier Ltd. This is an open access article under the CC BY-NC-ND license (<http://creativecommons.org/licenses/by-nc-nd/3.0/>).

Selection and Peer-review under responsibility of Physics Department, University of Namur.

**Keywords:** circular polarization; beetles; Mueller-matrix; polarimetric imaging

---

---

\* Corresponding author. Tel.: +33 1 44 27 40 85; fax: +33 1 44 27 39 82.

E-mail address: [serge.berthier@insp.jussieu.fr](mailto:serge.berthier@insp.jussieu.fr)

## Introduction

It is known for a long time now that many kinds of beetles, especially from the Plusiotis, Crysinae and Cetonidae families [1], and several other organisms such as shrimps, reflect a strongly circularly polarized light. It has also been observed that the larvae of few fireflies emit circularly polarized light [2]. In beetles, this effect is superimposed on the conventional thin film effects generating interference colours. The physical origin of this phenomenon has been clearly identified [3-5], but has long been considered as a curiosity, the interest for the organisms remaining mysterious. The situation has changed radically in 2008 when, for the first time, it has been shown that a shrimp *Ondotodactylus scyllarus*, producing this effect, was also able to detect this polarization state [6]. The principle of detection, as described by Chiou et al [6] consists in a complex arrangement of cells situated just behind the cornea and the crystalline cones of the ommatidies. A first layer of cells acts as a  $\frac{1}{4} \lambda$  retarder that converts a circularly polarized light in linear one. According to the direction of rotation of the incident light, two sets of cells, cross disposed, detect one or the other of these linear fields. Many studies were then undertaken, especially on Rutelinae and Cetonidae, to test their sensitivity to circular polarization, and attempt to discover the evolutionary interest. The results are mixed, some species being sensitive [7, 8], and other apparently not [9], despite a surprisingly high rate of polarization of the reflected light by structures otherwise relatively disordered. This mystery gives rise to many works and our intention, as physicist, is surely not to solve it but to provide basic elements for the study and characterization of natural optical phenomena involving the circular polarization of light.

In this article, first part will be devoted to theoretical background on the circular polarization. The second one on the circular polarization in nature: how it happens, where do we find it...? Finally the third part will be devoted to the various experimental techniques commonly used to characterize this state.

### 1. Theoretical recalls

Circular polarization state is somewhat uncommon in nature, however it is the ground state of the light. From a quantum view, the photon is indeed a particle of spin equal to 1, which can only have the values 1, 0, -1. The value 0 is forbidden due to the zero mass of the photon. It can only be found in two spin states  $\pm 1$ , which correspond in electromagnetism to the two states of left and right circular polarization. Any polarization state can then be represented as a linear combination of these two basic states. This is particularly the case of the linear polarization that can be represented as the sum of two counter rotating circular waves of the same intensity.

In the most general case, the Cartesian components of the actual displacement vector  $\mathbf{D}(z, t)$  of an electromagnetic wave propagating in any material may be written:

$$\begin{cases} D_x(z, t) = A_x \cos(\omega t - kz - \phi_x) \\ D_y(z, t) = A_y \cos(\omega t - kz - \phi_y) \end{cases} \quad (1)$$

In the plane wave, the extremity of the vector describes an ellipse known as Lissajous curve. This is the more general state for a monochromatic plane wave in a homogeneous medium. The direction of rotation of the ellipse depends on the phase difference  $\Delta\Phi = (\Phi_x - \Phi_y)$  between the two components. It is direct if  $\Delta\Phi$  is between 0 and  $\pi$  (left-handed), retrograde (right-handed) if it is between 0 and  $-\pi$ . Circular polarization is a particular state of light where the direction of the vector  $\mathbf{D}$  turns perpendicularly to the direction of propagation always maintaining the same module ( $D_x = D_y$ ) and where the phase shift  $\Delta\Phi$  between the two components is  $\pm (\pi / 2)$ .

There are several ways to experimentally produce such a wave. The conventional method is a transmission one. It consists in introducing a phase shift of  $\pi/2$  between the two orthogonal components of a linearly polarized wave. A birefringent plate of thickness suitably chosen, said  $\lambda/4$  or quarter-wave plate, with the axes parallel to the two components, is placed on the light path. After passing through, the component which has propagated in the high index medium is delayed by one quarter wavelength, thus phase-shifted by  $-\pi/2$ . Achromatic plates, thanks to the index dispersion of the material used, are now available that allow to cover relatively large frequency ranges.

## 2. Circular polarization in nature

### 2.1. Elliptical polarization by total reflection

In nature, the vast majority of the circularly polarized light concerns reflected light. The only purely physical origin, without the intervention of living organisms, involves the phenomenon of total reflection.

When passing through a high index  $n$  (generally water in nature) / low index  $n_0$  (air) dioptré, the wave is totally reflected for angles of incidence greater than the critical angle  $\theta_c$ , but the continuity conditions of normal and tangential components of the fields and potentials impose a phase difference at the reflection of the two polarization states  $s$  and  $p$ .

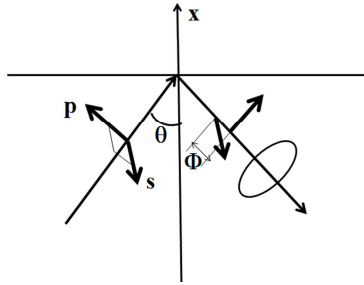


Fig. 1. Phase shift of the  $s$  and  $p$  waves after total reflection.

The component magnitudes are equal but they are obviously out of phase of an angle  $\Phi = \Phi_s - \Phi_p$ . The reflected wave is thus generally in an elliptical state. For incidence angles greater than the critical angle  $\theta_c$ , the reflection phase of each component is given by:

$$\begin{cases} \tan \Phi_s = \frac{n_0 \sqrt{\left(\frac{n}{n_0}\right)^2 \sin^2 \theta - 1}}{n \cos \theta} \\ \tan \Phi_p = \frac{n_0 \sqrt{\left(\frac{n}{n_0}\right)^2 \sin^2 \theta - 1}}{n_0 \cos \theta} \end{cases} \quad (2)$$

It implies a phase difference between the two waves given by:

$$\tan \frac{\Phi}{2} = \frac{\cos \theta \sqrt{\left(\frac{n}{n_0}\right)^2 \sin^2 \theta - 1}}{n \sin^2 \theta} \quad (3)$$

This phase shift, as a function of the incidence angle above the critical angle  $\theta_c$ , is shown in Fig. 2. It passes through a maximum  $\Phi_m$  for a particular angle  $\theta_m$  given respectively by:

$$\phi_m = 2 \operatorname{Arctan} \left( \frac{n^2 - n_0^2}{2n} \right) \quad \text{and} \quad \theta_m = \operatorname{Arctan} \left( \sqrt{\frac{2}{1+n^2}} \right) \quad (4)$$

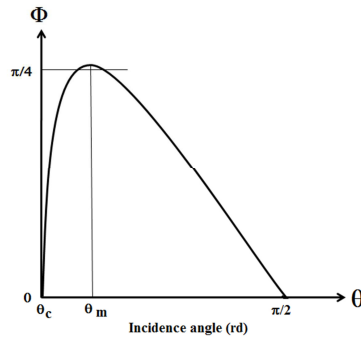


Fig. 2. Phase shift between the two s and p reflected waves as a function of the angle of incidence ( $n_0 = 1, n = 1.5$ ).

In the case of a dioptre water/air,  $\theta_m$  is of the order of  $60^\circ$  and the phase shift for this angle is  $32^\circ$ . In nature, this process requires an emerging wave that can be founded, for example, over shallow sandy bottom (beaches, lagoons ...).

So quite apart from this particular case that generally does not produce purely circular polarization (there should be a triple reflection in these conditions for a phase shift of  $\pi/2$  between the two components), all elliptical or circular states of light encountered in nature are generated by living organisms.

2.2. Polarization by reflection from chiral materials

As mentioned above, the other way to introduce a phase shift between two components of a plane wave is to make it pass through a uniaxial anisotropic material. Its permittivity tensor is given by:

$$\begin{bmatrix} \epsilon_x & 0 & 0 \\ 0 & \epsilon_x & 0 \\ 0 & 0 & \epsilon_z \end{bmatrix} = \begin{bmatrix} n_o^2 & 0 & 0 \\ 0 & n_o^2 & 0 \\ 0 & 0 & n_e^2 \end{bmatrix} \tag{5}$$

where  $n_o$  and  $n_e$  are the ordinary and extraordinary index. The component of the wave oriented along  $O_z$  will propagate at a different speed from that oriented along one of the others, and will be out of phase at the outlet of the material. We can then define a coefficient of phase delay:  $\beta = (n_o - n_e)k_o$  where  $k_o$  is the wave vector of the ordinary wave.

Depending on the sign of this coefficient the propagation medium is called positive or negative. The components of a wave oriented along these axes will be phase shifted in proportion to the distance traveled in the material and therefore the wave will emerge in a different state of polarization. There are several ways to connect these states thus to represent the effect of an optical system on an electromagnetic wave. In our case, the Mueller formalism is ideal because it connects light intensities that are experimentally measurable quantities. In this formalism, a state of light is characterized by four parameters that are grouped in a vector quantity with four components, the Stokes vector defined as:

$$S = \begin{bmatrix} P_0 \\ P_1 \\ P_2 \\ P_3 \end{bmatrix} = \begin{bmatrix} I_0 \\ I_x - I_y \\ I_{+45^\circ} - I_{-45^\circ} \\ I_L - I_R \end{bmatrix} \tag{6}$$

$I_0$  represents the total intensity of the wave,  $I_x, I_y, I_{+45}$  and  $I_{-45}$  the intensities of light linearly polarized along the axes and at  $45^\circ$  apart,  $I_L$  and  $I_R$  the intensities of components polarized circularly left and right. When crossing any

optical device, the Stokes vector undergoes a linear transformation represented by a real 4x4 matrix: The Mueller matrix. All the elements of the matrix represent measurable intensities and are defined as follow:

|           |                         |                         |                         |
|-----------|-------------------------|-------------------------|-------------------------|
| (OO)      | (XO-YO)/2               | (PO-MO)/2               | (LO-RO)/2               |
| (OX-OY)/2 | (XX+YY)/4-<br>(XY+YX)/4 | (PX+MY)/4-<br>(PY+MX)/4 | (LX+RY)/4-<br>(LY+RX)/4 |
| (OP-OM)/2 | (XP+YM)/4-<br>(XM+YP)/4 | (PP+MM)/4-<br>(PM+MP)/4 | (LP+RM)/4-<br>(LM+RP)/4 |
| (OL-OR)/2 | (XL+YR)/4-<br>(XR+YL)/4 | (PL+MR)/4-<br>(PR+ML)/4 | (LL+RR)/4-<br>(RL+LR)/4 |

The first letter of each pair represents the intensity of the incoming light, the second that of the out coming one. O is the total intensity of the wave, X, Y, P (+45°), M (-45°), L and R the intensities of the Stokes parameters, as defined above. So it takes 49 measurements of light intensity to completely determine the Mueller matrix of a linear optical system. The relationship between the emerging Stokes vectors  $S'$  and the incident one  $S$  being linear, the Mueller matrix  $M$  of an association of several components is the product of the matrices of each of these elements:

$$\mathbf{S}' = \mathbf{M} \cdot \mathbf{S} = \mathbf{M}_n \cdot \mathbf{M}_{n-1} \cdot \dots \cdot \mathbf{M}_1 \cdot \mathbf{S} \quad (7)$$

One can thus easily determine the characteristics of an outgoing wave from a stack of anisotropic layers. In the case of the beetles elytra of interest here, the layers are uniaxial anisotropic chitin plates which introduce a phase shift  $\Phi$  between the two components of a linear wave parallel to the axes. Their Mueller matrix is of the form:

$$\mathbf{M} = \begin{vmatrix} 1 & 0 & 0 & 0 \\ 0 & 0 & 0 & 0 \\ 0 & 0 & \cos\Phi & \sin\Phi \\ 0 & 0 & -\sin\Phi & \cos\Phi \end{vmatrix} \quad (8)$$

The elytra are formed by a stack of many layers of uniaxial anisotropic materials whose axes turn from one layer to the next one by a constant angle  $\theta$ . They form a "fan" filter, known as SOLC filter for which the Mueller matrix is the product of the individual matrix, each multiplied by the matrix of a rotator of angle  $\theta$  [10]:

$$\mathbf{M}' = \begin{vmatrix} 1 & 0 & 0 & 0 \\ 0 & \cos 2\theta & -\sin 2\theta & 0 \\ 0 & \sin 2\theta & \cos 2\theta & 0 \\ 0 & 0 & 0 & 0 \end{vmatrix} \quad (9)$$

It is then shown that the wave transmitted through such a filter is circularly polarized and that the direction of rotation depends on the relative values of the frequency, the rotation coefficient  $\alpha$  of the structure, given by:  $\theta = \alpha z$  and the sign of the phase coefficient  $\beta$ . The sign of  $\beta$  depends on the relative value of  $n_e$  and  $n_o$ . The direction of rotation of the reflected wave can then change for given wavelengths. The direction of rotation is thus likely to be reversed for particular frequencies, which is actually observed in some insects, as we shall see.

Another view of the phenomenon, less formal and more educational, also helps to explain this phenomenon. It is known that from a quantum point of view, a light wave is a flux of particles, the photons with energy  $E = h\nu$  and momentum proportional to the wave vector  $k = 2\pi/\lambda$ . The same reasoning is used to define the vector  $K$  of a periodic structure with path  $a$ :  $K = 2\pi/a$ . Conservation laws indicate that exchanges between light and matter are

made by multiple of this quantity, which involves opening gaps in the dispersion relation of the wave whenever  $k$  (wave) =  $NK$  (material). Any wave of frequency in these gaps cannot propagate in the structure and is therefore reflected.

Consider now a linearly polarized wave. As indicated above, such a wave is the sum of two waves right and left circularly polarized. When interacting with a cholesteric structure as that of beetles, the two components experience different media. The one with a rotator in phase with that of the structure sees a uniform index medium and propagates therein, the other that turns in countersense sees a periodic medium and will be in a photonic band gap whenever  $k = NK$ . It is thus reflected (Fig. 3). This phase matching between the rotators of the wave and the structure obviously depends on the respective frequencies and the direction of rotation of the reflected wave, thus varies periodically.

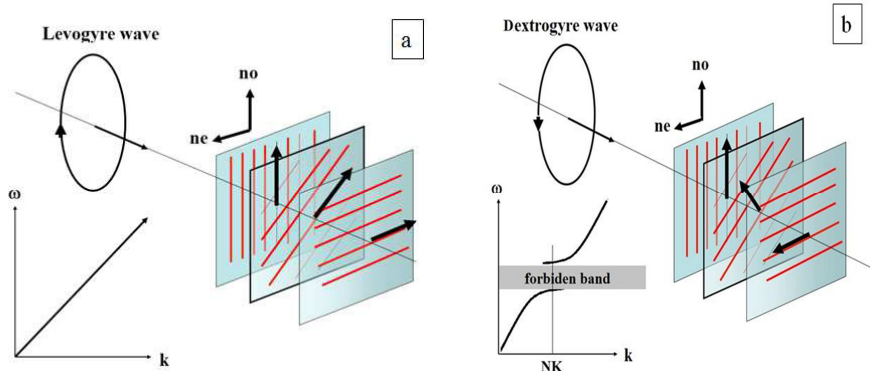


Fig. 3. (a) The field always sees the same refractive index  $n_o$ ; The wave propagates in the medium. (b) The field periodically sees two refractive indexes ( $n_o$  and  $n_c$ ). Waves of frequencies belonging to the band gap are reflected.

### 2.3 Light reflected by coleopteran elytra

The cuticle of arthropods and that of beetles, in particular, is a complex system with many layers and structures with very different properties. Layers of interest here form the exocuticle and are located near the surface, just below the various layers of protection (wax ...). Like all structures of insects, these layers are primarily composed of chitin [11].

The chitin molecule is a polysaccharide with a structure similar to vegetal cellulose. It is a long chain composed of monomers of N-acetylglucosamine. They are arranged in two or three rows forming an almost crystalline stick: the microfibrils. These sticks are embedded in a protein matrix. In a given layer, fibrils are roughly oriented parallel to each other and to the surface. Their orientation, the so called director, turns of a fixed angle from one layer to the following one. It results in a helicoidal structure similar to that of a liquid crystal in the cholesteric phase (Fig. 4.a).

In some species, these layers have a uniform thickness and produce relatively saturated colours by interference. In others on the contrary, their thickness is gradually evolving in the thickness of the cuticle, forming a Bragg mirror giving the insects a metallic appearance. In the first case, the rotation coefficient  $\alpha$  is fixed, it is a function of  $z$  in the second. The coefficient of phase delay  $\beta$  is more difficult to determine because the values of the index  $n_c$  and  $n_o$  are not precisely known. Note that if we accept the values determined for a butterfly (*Morpho menelaus*) [12],  $\beta$  changes sign for wavelength around 500 nm (Fig. 5.a), which implies a reversal of the direction of reflected wave rotation, as observed on *Chrysina argenteola* [13] and *Chrysina resplendens* (Fig. 5.b).

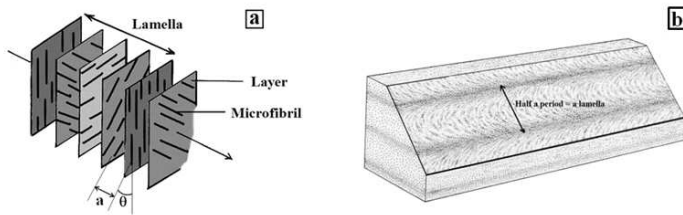


Fig. 4. (a) In a cholesteric phase, the director orientation regularly varies along the propagation axis. A period shows up when the director underwent a  $180^\circ$  rotation, determining thus a lamella. (b) An oblique section of the exocuticle exhibits arched structures characterizing cholesteric-type arrangement. Lamellae are formed by a  $180^\circ$  rotation of sticks.

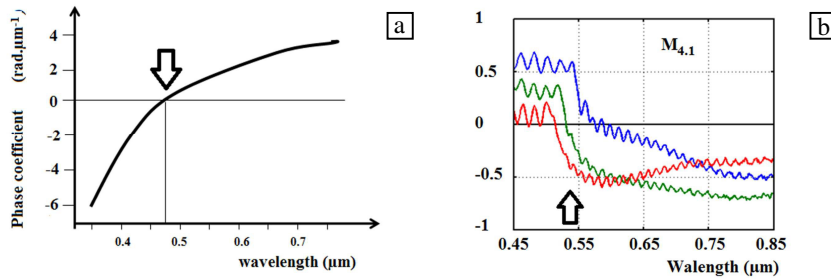


Fig. 5. (a) Phase coefficient  $\beta$  of birefringent chitinous film, deduced from the determination of the refractive index of the wings of *Morpho menelaus*. (b) Normalized  $M_{4,1}$  element of the Mueller matrix of *Chrysina resplendens*.

The geometry of the structure can be determined in several ways. Oblique thin sections present arrangement of arched structures which Bouligand and Neville [3-5] gave an explanation (Fig. 4.b). Knowing the cut angle, the geometry of the structure can be directly deduced from this pattern. Another method, also proposed by Bouligand and adapted by our group consists in polishing a convex portion of the elytra, making appear a series of concentric circles corresponding to different layers. After a light ion etching for excavating the proteinaceous material, may then be observed in each layer the orientation of the fibrils (Fig.6).

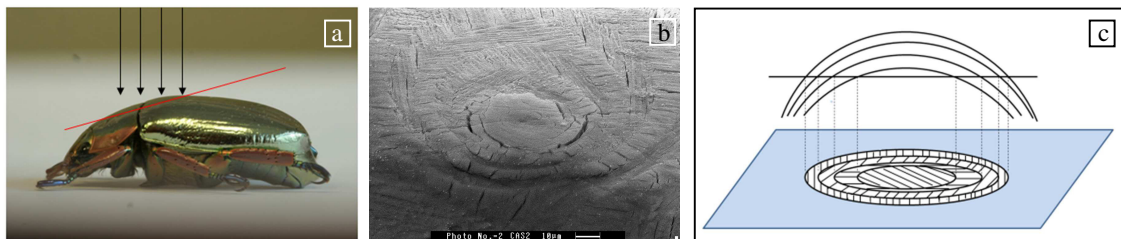


Fig. 6. Principle of the helicoidal structure determination. (a) *Chrysina resplendens*, lateral view; (b) SEM image of the polished elytra after ion etching; (c) Schematic representation (after Bouligand, 1969).

## 2.4 Other origins

**Emitted circularly polarized light** - The case is rare, but it has been shown that the light emitted by bioluminescence by the larvae of some fireflies is circularly polarized [2].

The larvae of *Photuris lucifrescens* and *Photuris versicolor* emit left-handed circularly polarized light by the left lantern and a right-handed one by the right one, which is a surprising exception, this axial symmetry having never been encountered in any other organism. The origin of this symmetry is unknown, as well as that of the circular



polarization. Two processes can be envisaged: either a chiral excited state is involved in the process of bioluminescence, or a circular dichroic medium absorbs a component of the emitted light. Again, the biological significance of the phenomenon is not clear. It is not known if these larvae are sensitive to this state of the light.

**Transmitted circularly polarized light** - The case is basically the same as above, only the light source is different. The light transmitted through various dinoflagellates is circularly polarized. The origin is to be found in the structured backbone of these organisms [14].

### 3. Optical characterization

#### 3.1. Ellipsometry

Any measure establishing linear relationships between the different states of the incident and emerging waves, from an optical device, can determine unambiguously the Mueller matrix of the system. One of the most widely used experimental techniques is ellipsometry [13, 15]. This highly accurate and well known method determines the spectral variations of each matrix element for different angles of incidence. Originally developed for the study of perfectly polished surfaces or thin films, the technique is very sensitive to the surface state of the material. Off specular measurements are now widespread and allow the study of scattering or anisotropic objects such as shells or insect wings. The principle of measurement is to determine the change of polarization state of a wave reflected from the sample surface. This change can be directly related to the optical and geometrical characteristics of the surface, making the ellipsometry a powerful tool for optical analysis of surfaces. The ratio of the two components  $r_s$  and  $r_p$  of a linearly polarized reflected wave is determined for various angles of incidence. It can be put under the form:

$$\rho = \frac{r_p}{r_s} = \tan\Psi e^{i\Delta} \quad (10)$$

The angles  $\Psi$  and  $\Delta$  or, more precisely  $\tan\Psi$  and  $\cos\Delta$ , are directly measured by ellipsometry. There are different types of ellipsometer, all based on the same principle illustrated in Fig. 7.

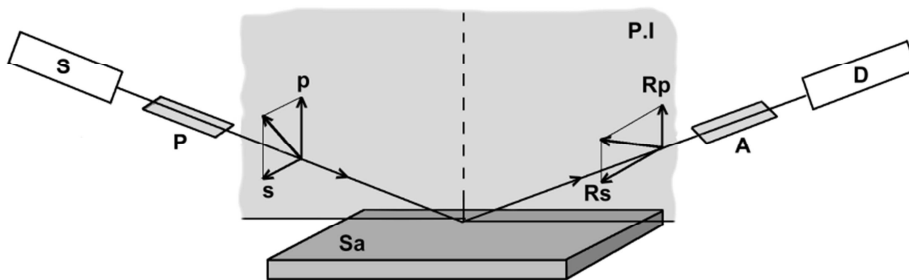


Fig. 7. Schematic of principle of an ellipsometer (Sa: sample, S: source, D: detector, P: polarizer, A: analyser). A polarizer and a compensator located on one arm of the ellipsometer, determine a defined state of the incident light polarization. An analyser and a detector located on the symmetrical arm, detect the change in polarization produced by reflection on the sample surface.

#### 3.2. Polarimetric imaging

Another method known as polarimetric imaging, whose principle is presented Fig. 8, allows spectral measurements as above (Fig. 9.a) but also to visualize the object under consideration for each element of the Mueller matrix, both in the real space as in the Fourier space [16-20]. In the latter, this approach provides information on the spatial dispersion of each polarization state after reflection on the object (Fig. 9.c). In real space,

it helps to know which part or component of the structure affects such element of the matrix (Fig. 9.b). 49 measurements are necessary to obtain a complete matrix.

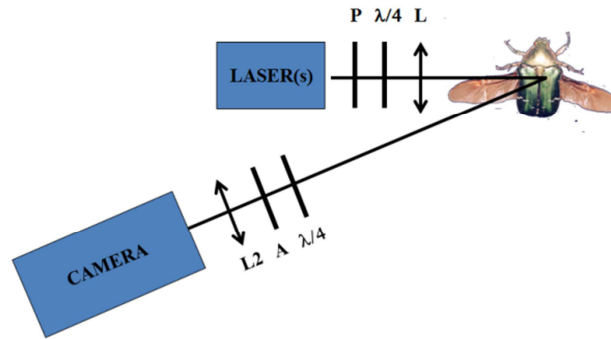


Fig. 8. Schematic representation of the polarimetric imaging. (P and A: polarizer and analyzer, L: Lens,  $\lambda/4$ : quarter wave plate).

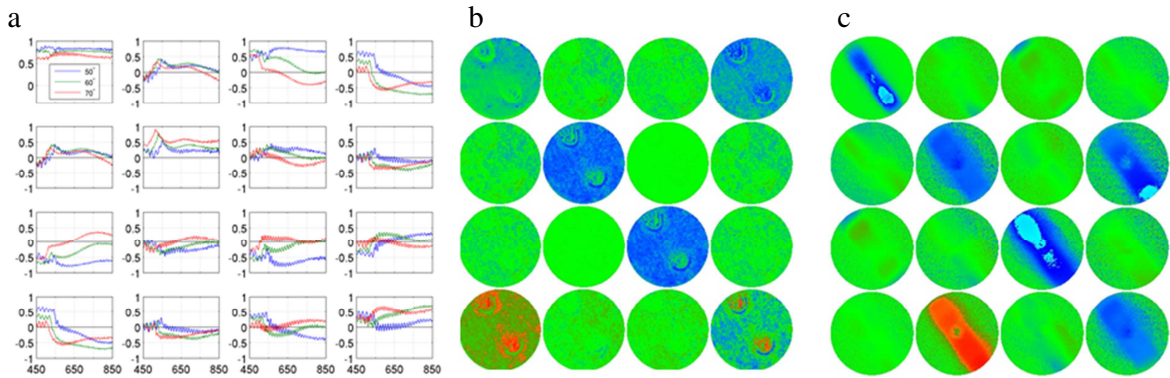


Fig. 9. Three modes of representation of the Mueller matrix. (a): Spectral representation for various angles. (*Chrysina replendens*,  $\theta = 50^\circ, 60^\circ, 70^\circ$ ); (b) image representation (*Cetonia aurata*); (c) Fourier representation (*Morpho menelaus*).

## Conclusion

Under the conditions and with the materials found in nature, only living organisms are capable of generating a circular polarization of light of high quality. The total reflection on an interface water/air does not induce sufficient phase shift in a single pass to achieve the optimum value of  $\pi/2$ . Circular or nearly circular polarization remains the prerogative of living beings and, for the vast majority, of insects. On the other hand, the sensitivity of some of these organisms to this polarization state has been demonstrated, even if the evolutionary interest is not yet clearly understood. In beetles, the appearance of the elytra is the result of not always independent optical phenomena. The helical organization of chitin layers of exocuticle generates both interference phenomena, responsible for the colour of the insect, and polarization effects here almost circular. These effects are interrelated, and the direction of rotation of the polarization depends on the frequency. For most of them, these insects are green and left-handed polarized at these frequencies. New analytical techniques, the generalized ellipsometry and polarimetric imaging allow an accurate determination of the spectral variations of each Mueller matrix element for different incidence angles. The polarimetric imaging allows to visualize the structural elements responsible for the effects observed and to determine the spatial distribution of the reflected waves. These analyses confirm the reversal of circular polarization for few species, as predicted by the theory. This complex phenomenon is mainly due to the reversal of the phase

factor sign of the structure. This factor is deduced from the values of the ordinary and extraordinary indices of the material. These indices are poorly known and should strictly be determined for each species.

### Acknowledgments

We wish to thank Antonello Di Martino, and Martin Foldyna (LPICM, Ecole polytechnique Palaiseaux) for the Imaging Polarimetric measurements on few scarabidae and butterflies. This work was supported by French state funds managed by the ANR within the Investissements d'Avenir programme under reference ANR-11-IDEX-0004-02, and more specifically within the framework of the Cluster of Excellence MATISSE.

### References

- [1] J.D. Pye, *J. Linnean Soc.* 100 (2010) 585–596.
- [2] H. Wynberg, E.W. Meijer, J.C. Hussmelen, H.P.S.M. Dekkers, P.H. Schppers, A.D. Carlson, *Nature* 286 (1980) 641–642.
- [3] Y. Bouligand, *CRAS* 2 (1985) 121–140.
- [4] Y. Bouligand, *J. de Phys.* 30 (1969) 90–103.
- [5] A.C. Neville, S. Caveney, *Biol. Rev.* 44 (1969) 53–562.
- [6] T.H. Chiou, S. Kleinlogel, T. Cronin, R. Caldwell, B. Loeffler, A. Siddiqi, A. Goldizen, J. Marshall, *Current Biology* 18 (2008) 429–434.
- [7] P. Brady, M. Cummons. *Am. Nat.* 175 (2010) 614–620.
- [8] E.J. Warrant, *Curr. Biol.* 20 (2010) R610–612.
- [9] M. Blaho, A. Egri, R. Hegedus, J. Josvai, M. Toth, K. Kentész, L.P. Biro, G. Kriska, G. Horváth. *Physiology&Behavior* 105 (2012) 1067-75.
- [10] S. Huard, in: *Polarisation de la lumière*, Masson, 1994, pp. 235–236.
- [11] R.F. Chapman, in: *The insects: Structures and functions*, Cambridges University Press, 1998, pp. 419–422.
- [12] S. Berthier, E. Charron, J. Boulenguez, *Insect Sci.* 13 (2006) 145–158.
- [13] H.G. Tompkins, E.A. Irene. *Handbook of Ellipsometry* William Andrew Publishing, Norwick (2005).
- [14] N. Shashar, T.W. Cronin, G. Johnson, L.B. Wolf, *Proc. Soc. Photo-Optical Instrumentation Engineers (SPIE)* 2426 (1995) 28–35.
- [15] H. Arwin, R. Magnusson, J. Landin, K. Jänendahl. *Philosophical Mag.* 92 (2012) 1583–1599.
- [16] R. Hegedüs, G. Szél, G. Horvath. *Vision Res.* 46 (2006) 2786–97.
- [17] Tatiana Novikova, Angelo Pierangelo, Sandeep Manhas, Abdelali Benali, Pierre Validire, Brice Gayet, Antonello De Martino, *Applied Physics Letters* 102 (2013) 241103.
- [18] Enric Garcia-Caurel, Antonello De Martino, Jean-Paul Gaston, Li Yan *Applied Spectroscopy* 67 (2013) 1–21.
- [19] Angelo Pierangelo, André Nazac, Abdelali Benali, Pierre Validire, Henri Cohen, Tatiana Novikova, Bicher Haj Ibrahim, Sandeep Manhas, Clément Fallet, Maria Rosaria Antonelli, Antonello De Martino, *Optics Express* 21 (2013) 14120.
- [20] Enric Garcia-Caurel, Razvigor Ossikovski, Martin Foldyna, Angelo Pierangelo, Antonello De Martino, Bernard Drévilion, *Ellipsometry at the nanoscale*, Springer, 2013, pp. 31.
- [21] Tatiana Novikova, Angelo Pierangelo, Antonello De Martino, Abdelali Benali, Pierre Validire, *Optics and Photonics News* October 2012.